

# Verification of a coupled climate-hydrological model against Holocene palaeohydrological records

Philip J. Ward<sup>a,\*</sup>, Jeroen C.J.H. Aerts<sup>b</sup>, Hans de Moel<sup>b</sup>, Hans Renssen<sup>a</sup>

<sup>a</sup> Department of Palaeoclimatology and Geomorphology, Faculty of Earth and Life Sciences, Vrije Universiteit Amsterdam, De Boelelaan 1085, 1081 HV Amsterdam, The Netherlands

<sup>b</sup> Institute for Environmental Studies, Faculty of Earth and Life Sciences, Vrije Universiteit Amsterdam, De Boelelaan 1085, 1081 HV Amsterdam, The Netherlands

Received 6 June 2006; received in revised form 11 December 2006; accepted 18 December 2006

Available online 22 December 2006

## Abstract

We have coupled a climate model (ECBilt-CLIO-VECODE) and a hydrological model (STREAM) offline to simulate palaeodischarge of nineteen rivers (Amazon, Congo, Danube, Ganges, Krishna, Lena, Mackenzie, Mekong, Meuse, Mississippi, Murray–Darling, Nile, Oder, Rhine, Sacramento–San Joaquin, Syr Darya, Volga, Volta, Zambezi) for three time-slices: Early Holocene (9000–8650 BP), Mid-Holocene (6200–5850 BP) and Recent (1750–2000 AD). To evaluate the model's skill in retrodicting broad changes in mean palaeodischarge we have compared the model results with palaeodischarge estimates from multi-proxy records. We have compared the general trends inferred from the proxy data with statistical differences in modelled discharge between the three periods, thereby developing a technique to assess the level of agreement between the model and proxy data. The quality of the proxy data for each basin has been classed as good, reasonable or low. Of the model runs for which the proxy data were good or reasonable, 72% were in good agreement with the proxy data, and 92% were in at least reasonable agreement. We conclude that the coupled climate-hydrological model performs well in simulating mean discharge in the time-slices studied. The discharge trends inferred from the proxy and model data closely follow latitudinal and seasonal variations in insolation over the Holocene. For a number of basins for which agreement was not good we have identified specific mechanisms which could be responsible for the discrepancy, primarily the absence of the Laurentide ice sheet in our model. In order to use the model in an operational sense within water management studies it would be useful to use a higher spatial resolution and a daily time-step.

© 2006 Elsevier B.V. All rights reserved.

*Keywords:* coupled climate-hydrological model; palaeodischarge; global rivers; Holocene; model validation; insolation

## 1. Introduction

Climate is the principal driving force of hydrological systems and even modest climate changes have the potential to cause significant changes in hydrological

processes (Knox, 2000, 2003), including changes in the volume and temporal distribution of river discharge (Van Deursen, 1995). An understanding of these changes is of utmost importance since future climate change may alter both flood and drought characteristics of river systems (Meybeck, 2003).

In order to plan for these changes quantitative data are required on both long-term average discharge and the changes in frequency and intensity of low and peak flows

\* Corresponding author. Tel.: +31 20 59 87144; fax: +31 20 59 89941.  
E-mail address: [philip.ward@falw.vu.nl](mailto:philip.ward@falw.vu.nl) (P.J. Ward).

(Aerts and Droogers, 2004). To provide these estimates simulated future climate data can be used as input for hydrological models, which can then be utilised to project future changes in discharge regimes. Numerous attempts have been made to develop such models at the global scale (e.g., Yates, 1997; Klepper and Van Drecht, 1998; Vörösmarty et al., 1998; Arnell, 1999; Alcamo et al., 2003; Döll et al., 2003), and at the individual basin level (see e.g., Arnell et al., 2001, p. 203, and references therein). To provide projections of future discharge such models are validated by comparing their output to observed data on past discharge from gauging stations. However, even the longest instrumental records are too short to adequately evaluate long-term and large ranges of potential climatic variations (Chatters and Hoover, 1986; Ely et al., 1993; Knox, 2000).

Studies of palaeodischarge provide a means to overcome this lack of long-term observed data by providing a dataset for the validation of model response over periods of thousands of years. To date few studies have been carried out to model palaeodischarge based on palaeoclimatic data. Coe and Harrison (2002) used runoff fields derived directly from an AGCM (Atmospheric General Circulation Model) in combination with a river routing algorithm to simulate lake level changes in northern Africa at ca. 6 ka. BP. At the basin scale the use of runoff data derived directly from AGCMs has the disadvantage that runoff fields are less well resolved than climatic fields. Research using climatic output from climate models, coupled with hydrological models, to specifically simulate Holocene river discharge, remains elusive.

The main goal of our study is to develop a coupled climate-hydrological model for simulating Holocene discharge. The study involves the offline coupling of the climate model ECBilt-CLIO-VECODE and the hydrological model STREAM. This is achieved through the following means:

1. set up and calibrate the model for the Recent period for nineteen rivers;
2. model the discharge of these rivers during three time-slices in the Holocene;
3. identify independent proxy data on Holocene discharge for these rivers;
4. evaluate the model's ability to simulate the main trends in changes of palaeodischarge magnitude.

We view the offline coupling of the climate and hydrological models as a first step; the ultimate aim is to couple these models online.

## 2. Methods

In this study we compare simulated river discharges to proxy records of palaeodischarge for three time-slices in the Holocene, namely 9000–8650 BP (Early Holocene), 6200–5850 BP (Mid-Holocene) and 1750–2000 AD (Recent). The abbreviations EH, MH and RT are used respectively to refer to these time-slices. The period 9000–8650 BP was selected since it represents the time-period in which seasonal and latitudinal anomalies in insolation values compared to present were near the Holocene maximum (Berger, 1978). The

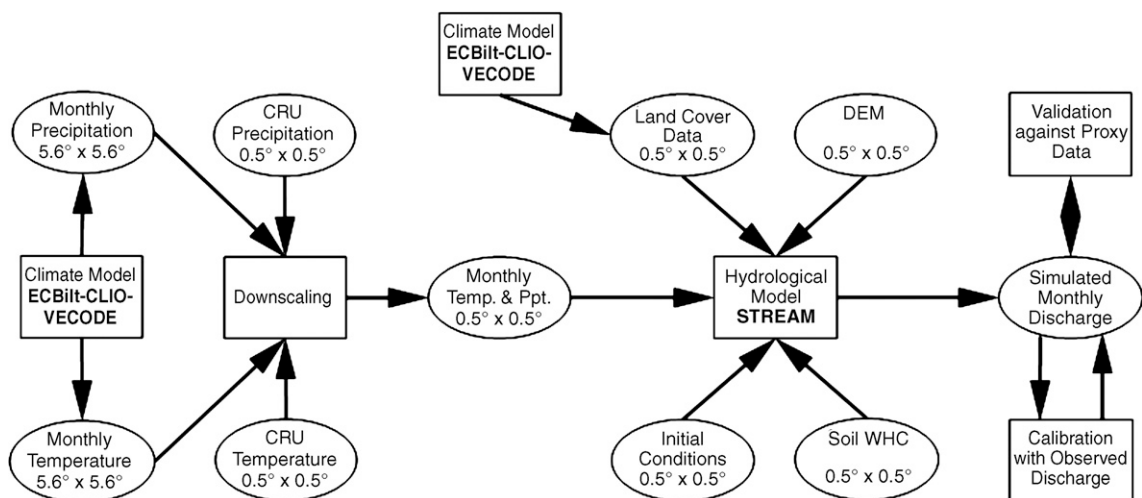


Fig. 1. Flowchart of the research approach and methodology used in this study.

period 6200–5850 BP represents a period with seasonal differences in insolation between those of 9000–8650 BP and present. Furthermore, the latter period is used as a standard reference period for comparing model and proxy data, e.g. The Project for Intercomparison of Land-Surface Parameterization Schemes (PILPS: [Henderson-Sellers et al., 1996](#)). The research approach is shown schematically in [Fig. 1](#).

The climate data used as input in the hydrological model were derived from a 9000 yr experiment using ECBilt-CLIO-VECODE ([Renssen et al., 2005a](#)). As the hydrological model, STREAM ([Aerts et al., 1999](#)), was run at a finer spatial resolution than ECBilt-CLIO-VECODE, a downscaling step was implemented. Nineteen basins were selected for modelling ([Fig. 2](#)), based on their geographical distribution and on the availability of palaeodischarge proxy data. Given the resolution of the hydrological model ( $0.5^\circ \times 0.5^\circ$ ), only medium or large basins were modelled, with the exception of the Meuse (ca. 33 000 km<sup>2</sup> ([Pfister et al., 2004](#))). Whilst this basin is relatively small and represented by just two grid cells in the climate model, and fourteen grid cells in STREAM, it will be examined at a higher resolution in a forthcoming project; hence it was included in this study.

### 2.1. Climate model and Holocene climate experiment

ECBilt-CLIO-VECODE is a three-dimensional coupled climate model consisting of three components describing the atmosphere, ocean and vegetation. The atmospheric component (ECBilt2) is a T21, 3-level quasi-geostrophic model ([Opsteegh et al., 1998](#)). The ocean–sea–ice component (CLIO) consists of an ocean

general circulation model coupled to a thermodynamic–dynamic sea–ice model ([Goosse and Fichefet, 1999](#)). The final component is VECODE, a dynamic vegetation model which simulates the dynamics of two main terrestrial plant types (forest and grasses) as well as bare soil, in response to climatic fluctuations ([Brovkin et al., 2002](#)). In ECBilt-CLIO-VECODE the simulated vegetation covers only affect the land-surface albedo, but do not influence other processes such as soil hydrology ([Goosse et al., 2005](#)). ECBilt is an Earth System Model of Intermediate Complexity (EMIC) (see [Claussen et al., 2002](#)), and runs two orders of magnitude faster than most Comprehensive General Circulation Models ([Opsteegh et al., 1998](#)). It was therefore possible to model the Holocene in a transient run, allowing for states of non-equilibrium in the climate ([Renssen et al., 2005a](#)).

The output of ECBilt-CLIO-VECODE used in this study were derived from a 9000 yr long experiment forced by annually varying orbital parameters and atmospheric greenhouse gas concentrations (CO<sub>2</sub> and CH<sub>4</sub>) ([Renssen et al., 2005a](#)). Besides these external forcings several internal feedback mechanisms play an important role, especially albedo feedbacks. However, the deglaciation of the Laurentide ice sheet in the early Holocene was not considered. In the experiment used here ([Renssen et al., 2005a](#)), a number of important shorter term forcing mechanisms are not included, especially fluctuations in solar activity and volcanic aerosol content. Thus the forcing parameters effect long-term (millennial) climatic fluctuations; as a result short-term discharge fluctuations will be difficult to detect. However, as the aim of our study is to assess the model's ability to retrodict broad changes in palaeodischarge magnitude the long-term signal is of particular use. The



[Fig. 2](#). World map showing the rivers modelled in this study. The GIS map was constructed by [Renssen and Knoop \(2000\)](#) and was used in the hydrological model to set the boundaries of the modelled basins.

atmospheric component of ECBilt-CLIO-VECODE has a spatial resolution of ca.  $5.6^\circ \times 5.6^\circ$  and a monthly output interval. Because of this low spatial resolution and the relatively simple atmospheric physics, the model is unable to capture El Niño Southern Oscillation (ENSO) variability, which may have been different during the Holocene than today (Moy et al., 2002). However, since we are examining the mean long-term discharge trends over 250–350 yr time-slices, decadal variations in discharge are not analysed. Given the quasi-geostrophic nature of the model, climates in tropical regions are generally less well resolved than those in other regions (Goosse et al., 2005).

## 2.2. Hydrological model

STREAM (Spatial Tools for River Basins and Environment and Analysis of Management Options) is a grid-based spatially distributed water balance model that describes the hydrological cycle of a drainage basin as a series of storage compartments and flows (Aerts et al., 1999). It is based on the RHINEFLOW model of Kwadijk (1991, 1993). STREAM calculates the water balance per grid cell using the Thornthwaite equations for potential evapotranspiration (Thornthwaite, 1948) and the Thornthwaite and Mather equations for actual evapotranspiration (Thornthwaite and Mather, 1957). The main flows and storage compartments used to calculate water availability per grid cell are shown in Fig. 3. The direction of water flow between grid cells is based on a digital elevation model (DEM). STREAM or RHINEFLOW have been successfully applied to numerous basins of varying size and in different regions.

In this study we have run STREAM at a spatial resolution of  $0.5^\circ \times 0.5^\circ$  using a monthly time-step. This

resolution was selected for a number of reasons. As one of the objectives of our study is to assess the model's ability to simulate the main trends in changes of palaeodischarge magnitude, a daily time-step was deemed inappropriate as the palaeodischarge proxy data do not give indications of daily flows. Furthermore, running the model on a global scale with a daily time-step would be computationally too demanding. The choice of the spatial resolution was based on similar considerations. Moreover, the Climate Research Unit (CRU) of the University of East Anglia has created a gridded-set of observed climate variables for the globe at a  $0.5^\circ \times 0.5^\circ$  resolution (CRU TS 2.0) (Mitchell et al., 2003), which has been found to be useful for the downscaling of climate model data to regional resolutions (Bouwer et al., 2004).

## 2.3. STREAM input data

We have created a raster GIS database with all maps digitised to a  $0.5^\circ \times 0.5^\circ$  resolution. In this section a summary of the input data sources is given.

### 2.3.1. Climate data

The climate data (mean monthly temperature and precipitation) were derived from ECBilt-CLIO-VECODE, and were subsequently downscaled to the resolution of the STREAM model. The first step was a spatial downscaling procedure (Bouwer et al., 2004), whereby the values from the ca.  $5.6^\circ \times 5.6^\circ$  climate model grid were resampled onto a  $0.5^\circ \times 0.5^\circ$  grid. The spatially downscaled climate maps have a resolution of  $0.5^\circ \times 0.5^\circ$ , but only reflect spatial variability at the scale of the climate model ( $5.6^\circ \times 5.6^\circ$ ), which is too coarse for direct use in (regional) hydrological studies (Arnell et al., 1996; Wood et al., 2002, 2004; Bouwer et al., 2004; Kleinn et al., 2005). Therefore a second downscaling step is required to introduce a more realistic and greater degree of spatial variability. There are two main approaches to downscaling climate model data: statistical methods (e.g., Wilby and Wigley, 1997; Wilby et al., 1998; Wood et al., 2002; Bouwer et al., 2004) and dynamical approaches using regional circulation models (RCMs) nested within the coarser climate model (e.g., Cocke and LaRow, 2000; Kim et al., 2000; Murphy, 2000; Yarnal et al., 2000; Wood et al., 2002). The results of these two approaches have been found to have similar levels of skill (e.g. Wilby et al., 2000; Wood et al., 2004) but dynamical methods are computationally far more demanding (Bouwer et al., 2004). The scale of our study renders this approach prohibitive, since the global spread of basins would

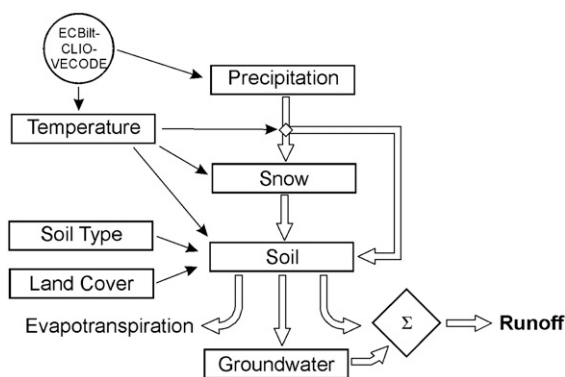


Fig. 3. Water balance storage compartments and flows in the STREAM model (adapted from Aerts et al., 1999).

necessitate the nesting of several RCMs into ECBilt-CLIO-VECODE.

Statistical downscaling involves the use of correction factors (for temperature additive and for precipitation multiplicative) which are applied to the low resolution modelled data so as to preserve the statistical properties of a higher resolution observed climate dataset (Bouwer et al., 2004). In our study this approach was problematic because in some areas very large correction values would have been necessary. This would have been the case especially in arid areas where very high correction factors based on current precipitation patterns would have been transferred to other periods in the Holocene. For instance it is known that the Sahel received much more precipitation than today during parts of the Holocene, and at times would have been covered by grasses (Roberts, 2002; Renssen et al., 2003). Using a very high correction factor (based on current arid Sahel conditions) to downscale EH precipitation data would result in arid conditions whilst this was not the case.

Therefore, we devised a new redistribution technique. Observed monthly temperature and precipitation data at a  $0.5^\circ \times 0.5^\circ$  resolution were obtained for the baseline period 1961–1990 from the CRU TS 2.0 dataset (Mitchell et al., 2003). The mean observed temperature and precipitation values were upscaled to the resolution of ECBilt-CLIO-VECODE simply by calculating the mean values of all high-resolution cells belonging to the corresponding  $5.6^\circ \times 5.6^\circ$  grid cell. The differences between the observed temperature and precipitation values at the lower and the higher resolution were then calculated, thereby creating correction factors on a  $0.5^\circ \times 0.5^\circ$  grid. Subsequently these correction values were applied to the spatially downscaled ECBilt-CLIO-VECODE data. Using this approach the total precipitation and average temperature simulated by ECBilt-CLIO-VECODE are redistributed over the higher resolution grid cells according to the present day spatial distribution, whilst the absolute values at the resolution of ECBilt-CLIO-VECODE remain unchanged. Hence, temperature and precipitation gradients resulting from differences in relief and distance from the oceans are better represented in the climate data. This approach assumes that the present day regional distribution of temperature and precipitation was the same during the Holocene time-slices studied. In reality this is not the case since climatic patterns change (IPCC, 2001). However as Kleinn et al. (2005) indicate, for catchments of several thousand square-kilometres and for runoff evolution on a monthly timescale, catchment mean precipitation is the most

important factor for river discharge whilst the finer scale distribution within the catchment is less important.

### 2.3.2. Soils and hydrography

A crop factor (Crop F) map is used in STREAM for the calculation of potential evapotranspiration based on the Thornthwaite (1948) equations. The crop factor map used in this study for 1750–2000 AD was based on a map of land cover characteristics from the WARibaS project (Klepper and Van Drecht, 1998), and was reclassified to crop factors based on land use co-efficients listed in Van Deursen and Kwadijk (1994) and Aerts and Bouwer (2002). For the EH and MH, the anomalies between the VECODE output for those time-slices and the VECODE output for the Recent time-slice were calculated, and then reclassified to crop factor anomalies. These anomalies were then reconciled with the modern crop factor map to create crop factor maps for the palaeo time-slices. As such, only land cover changes resulting from natural climatic change are used to force the hydrological model. The simulated change in basin averaged crop factor between the time-slices is very low in most cases. A change in basin-wide palaeo crop factor of more than 5% (compared to RT) was only registered for the following basins and time-slices: Krishna, EH (+6.6%); Nile, MH (+6.5%), EH (+13.0%); Syr Darya, EH (+6.0%). Hence, for the majority of basins studied the simulated effects of land cover changes on evapotranspiration will be low.

A map showing the water holding capacity (WHC) of the soil is used by STREAM in the calculation of evapotranspiration, direct runoff, groundwater seepage and baseflow. In this study the WHC map was taken from the WARibaS project (Klepper and Van Drecht, 1998), and was used for all three time-slices. Changes in soil types during the Holocene are therefore not included in this study.

The flow direction map of Renssen and Knoop (2000) was used to determine the direction of water flow between grid cells in STREAM. This map was constructed by determining water flow direction based on the TerrainBase DEM of the National Geophysical Data Center (NGDC, 1997). The resulting map was compared with data on the location of major river basins from the ArcWorld database (ESRI, 1992); the similarity was good (Renssen and Knoop, 2000).

To obtain realistic initial conditions for soil water storage, groundwater storage, snow cover and accumulated potential water loss (init maps) we adopted a perpetual simulation technique (Kleinn et al., 2005). Prior to commencing model calibration the init maps were assigned dummy values (the results of previous

test runs). The model was then run for a period of 50 yrs (i.e. 600 iterations), and the output maps for these parameters after the final iteration were used as input init maps.

### 2.3.3. Discharge data

Data for the Nile were taken from Hurst et al. (1946), as cited in Hipel and McLeod (1994). TU Delft provided observed data for the Zambezi. The discharge data for the other rivers were taken from the RivDis database (Vörösmarty et al., 1998), except for those for 1984–1999 for the Congo, which were taken from the SAGE river discharge database (<http://www.sage.wisc.edu/riverdata/>). The gauging station locations and the periods for which calibration was carried out can be found in the Appendix.

### 2.4. Calibration and validation of STREAM

We carried out the calibration of STREAM by varying model parameters with the aim of reproducing annual and monthly discharge characteristics similar to those in the observed record. A similar approach has been successfully employed in numerous studies (e.g., Wood et al., 2002; Christensen et al., 2004). The parameters used for calibration are CropF; WHC; HEAT (used in the Thornthwaite (1948) equation for calculating potential evapotranspiration); TOGW multiplier (determines the proportion of surplus water per grid cell that runs off directly or that seeps to the groundwater); C factor (determines the proportion of groundwater that contributes to baseflow); Melting (determines the rate of snowmelt when temperature is above a critical value) (for a more detailed description see Kwadijk (1993)). For all of the basins it was assumed that precipitation would fall as snow below a temperature of 0 °C (e.g., Kwadijk, 1993). The only basin where a different value was used was the Syr Darya, where this was set to 2 °C to compensate for an overestimation of winter temperatures by ECBilt-CLIO-VECODE in this region.

The downscaled ECBilt-CLIO-VECODE climate data were used as input for the calibration (as opposed to observed climate data) since the palaeodischarge simulations were also carried out using these data. Hence, the discharge series forced by the climate model only reflect discharge trends and not actual monthly or annual discharges (i.e. a wet month in the observed data does not per se correspond to a wet month in ECBilt-CLIO-VECODE). It was therefore only possible to compare the monthly means of discharge over the whole calibration period, and not the paired means of individual

months or years. Calibration was carried out for as long a period as possible, the length being primarily determined by the availability of observed discharge data and secondarily by the construction of major dams. No corrections have been made for minor dams, since data on their effects on river discharge are scarce.

A more physically based approach to parameter estimation is of course desirable, but observed data on factors like groundwater storage, proportion of surplus water to runoff or groundwater seepage are limited. Nevertheless, STREAM does simulate monthly data on changes in soil–water storage, groundwater and snow cover (results not shown here). Although these results were not compared with independent observed data they did remain in equilibrium over the calibration period.

The agreement between modelled and observed discharge was in the first case assessed by visual inspection of the annual hydrographs. The agreement of the total annual discharge was assessed by expressing the mean annual observed discharge as a percentage of the mean annual modelled discharge (total accuracy, %). The correlation of the paired means of monthly discharge was assessed using the Pearson Product Moment Correlation Co-efficient,  $r$  (Legates and McCabe, 1999), and the co-efficient of efficiency,  $E$  (Nash and Sutcliffe, 1970). The calibration results and parameters used are listed in the Appendix.

Hydrographs are presented here for those rivers with the poorest agreement according to the statistical analysis: Congo, Murray–Darling and Rhine (Fig. 4). Whilst there is some discrepancy in the temporal distribution of discharge between modelled and observed data, the general pattern has been preserved. In all three cases the total accuracy of the annual total discharge is very good.

### 2.5. Assessment of agreement between modelled discharges and proxy data

To validate the simulated Holocene discharge results we compared our simulated discharges with multi-proxy records of palaeohydrology obtained through an extensive review of published literature. For each basin we firstly assessed the quality of the proxy data (good, reasonable, low), in terms of the confidence that they reflect the actual palaeodischarge situation of the river in question during the relevant time-slice. Whilst such an assessment is somewhat subjective, we used three criteria for standardisation:

1. Does at least one of the proxy records refer specifically to the basin in question?

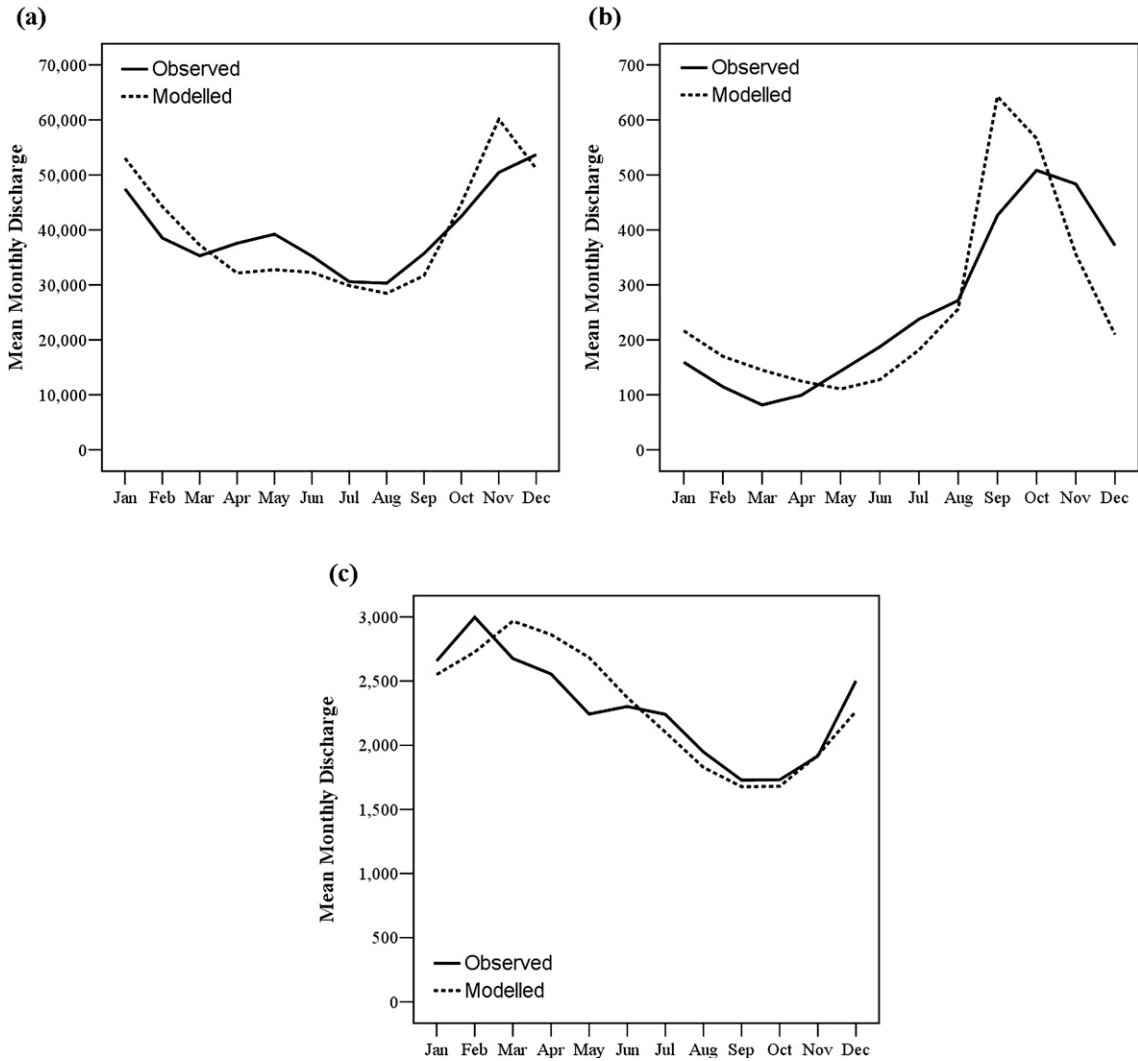


Fig. 4. Hydrographs of observed and calibrated model discharge ( $\text{m}^3 \text{s}^{-1}$ ) for the three basins with the poorest agreement according to the statistical analysis: (a) Congo, (b) Murray–Darling, (c) Rhine.

2. Does at least one of the proxy records explicitly examine river discharge?
3. Are there multiple proxy records giving the same signal of palaeodischarge?

In principle where all three of the criteria were met we classed the proxy quality as good, where two or more were met as reasonable, and otherwise low.

Thereafter we developed and applied two tests to assess the level of agreement between the modelled and proxy discharge data. Agreement is said to be good when both of these tests are passed, reasonable when one is passed, and low when neither is passed:

*Mean test:* This test examines whether the relative change between modelled mean annual discharge in the

RT time-slice and the palaeo time-slices is in agreement with the direction of change inferred from the proxy data. Where the proxy data suggest a relative increase or decrease in discharge in relation to the RT time-slice, the modelled data are in agreement when the latter indicate the same direction of change. For those basins for which the proxy data suggest that palaeodischarge was similar to the RT time-slice, we define similar in the modelled discharge as a relative change between the RT and palaeo time-slices of less than 10%.

*Variability test:* This test assesses whether the relative change of modelled mean annual palaeodischarge in relation to that of the RT time-slice falls outside the variability around the mean of the latter, and if so whether this change is in agreement with the proxy data. Firstly we calculated whether the modelled mean

palaeodischarge fell within or outside 2 standard deviations ( $2\sigma$ ) of RT 10-yearly mean annual discharge. We used a 10-year mean due to the high degree of interannual variability in river discharge. In palaeoclimatic studies it is common to use 30-year means for such assessments, but this was not appropriate here given the relatively short span of the RT time-slice (250 yrs). Where the proxy data infer a relative increase or decrease of palaeodischarge compared to RT, agreement was conferred where the mean monthly modelled palaeodischarge fell outside  $2\sigma$  of mean monthly RT modelled discharge. Where the proxy data infer palaeodischarge similar to that of the RT time-slice, agreement was conferred where the mean monthly palaeodischarge fell within  $2\sigma$  of the mean monthly RT discharge.

### 3. Results

The modelled mean monthly discharges for each basin for the RT time-slice are shown in Table 1. For the EH and MH, modelled discharges are given as percentage changes relative to RT discharge. Similarly, palaeodischarges inferred from the proxy data are indicated as relative changes in direction compared to the RT time-slice (+/=/-). The specific proxy data used in the model-proxy comparison are discussed in Section 4.1. The use of ‘++’ indicates that the relative magnitude of change in the EH is greater than that in the MH, according to the proxy data. In the first column of Table 1 the basins are grouped according to the quality of the proxy data (good, reasonable, low). No clear signal was observed for the EH Sacramento–San Joaquin since the

Table 1  
Comparison of modelled discharge and discharge implied from the proxy data

Basin	Recent (RT)		Mid-Holocene (MH)			Early Holocene (EH)		
	Modelled mean annual discharge ( $\text{m}^3\text{s}^{-1}$ )	$2\sigma$ of 10-year mean discharge (%)	Modelled discharge (% change on Recent)	Proxy +/=/-	Agreement	Modelled discharge (% change on Recent)	Proxy +/=/-	Agreement
<i>Proxy data quality</i>								
<i>Good</i>								
Amazon	152517	3.5	-0.7 †	-	Reasonable	-2.4 †	-	Reasonable
Ganges	10528	8.4	+7.2 †*	=/+	Good	+30.2 † *	++	Good
Congo	36589	7.1	+11.7 † *	+	Good	+12.1 † *	++	Good
Nile	2554	9.5	+10.9 †*	+	Good	+22.1 † *	++	Good
Sacramento–San Joaquin	658	33.8	-1.0 † *	=	Good	+9.1	?	N/A
Danube	6557	19.4	+8.1 † *	=	Good	+12.5 *	=	Reasonable
Lena	16714	7.6	-0.5 † *	=	Good	-3.4 † *	=	Good
<i>Reasonable</i>								
Krishna	1714	18.4	+7.8 †	+	Reasonable	+26.4 † *	+	Good
Volta	1248	13.1	+48.3 † *	+	Good	+73.3 † *	++	Good
Oder	527	15.7	+1.7 † *	=	Good	-0.6 † *	=	Good
Mississippi	15617	29.8	+3.1 †	+	Reasonable	+5.7	-	Poor
Syr Darya	547	N/A	+19.6 †	+	Good <sup>1</sup>	+58.0 †	+	Good <sup>1</sup>
Mackenzie	8928	9.9	-3.8 † *	=	Good	-14.5	+	Poor
<i>Low</i>								
Mekong	732	N/A	+12.8 †	+	Good <sup>1</sup>	+34.8 †	++	Good <sup>1</sup>
Zambezi	445	31.4	-44.8	+	Poor	-60.7	+	Poor
Murray–Darling	221	N/A	+3.5 †	+	Good <sup>1</sup>	-20.2 †	-	Good <sup>1</sup>
Rhine	2239	8.2	0 † *	=	Good	+0.6 † *	=	Good
Meuse	319	8.1	+2.6 † *	=	Good	+4.5 † *	=	Good
Volga	7929	10.3	+8.0 † *	=	Good	+6.2 †	+	Reasonable

In the left-hand column the basins are subdivided according to the quality of the proxy data (good, reasonable, low). The MH and EH modelled discharges are expressed as percentage changes in relation to the RT time-slice. The proxy data infer a relative change in direction in relation to the RT time-slice. † indicates that the model and proxy data are in agreement according to the mean test; \* indicates that the model and proxy data are in agreement according to the variability test. Proxy and model agreement is said to be good when both of these tests are passed, reasonable when one of the tests is passed, and poor when neither is passed. <sup>1</sup> The variability test has not been applied to the Syr Darya, Murray–Darling or Mekong, since their mean monthly discharge frequencies are not normally distributed. The degree of agreement has been established on the basis of the mean test only (pass=good/fail=poor).

proxy records give contradictory evidence. Proxy-model agreement according to the mean test is indicated in Table 1 by the symbol †, whilst agreement according to the variability test is indicated by the symbol \*. The variability test has not been applied to the Syr Darya, Murray–Darling or Mekong, since their mean monthly discharges are not normally distributed.

In total 73% of the palaeodischarge simulations were in good agreement with the proxy data, and 89% were in at least reasonable agreement. For the basins for which good proxy data were available, 77% of the runs simulated discharge in good agreement with the proxy data, and all of the runs simulated discharge in good or reasonable agreement. If we combine the basins for which good and reasonable proxy data were available, then 72% of the simulated palaeodischarge runs were in good agreement with the proxy data, and 92% were in good or reasonable agreement.

The proxy records also suggest that the relative magnitude of mean annual discharge was greater in the EH than in the MH for five of the rivers studied: Ganges, Congo, Nile, Volta and Mekong. For all of these rivers our model simulates lower mean annual discharge in the MH compared to the EH. Hence our model not only simulates well the relative changes in discharge magnitude between the present day and the palaeo time-slices, but also the relative changes of discharge magnitude between the two palaeo time-slices studied.

## 4. Discussion

### 4.1. Zonal assessment of model and proxy data

For the Holocene time-slices, orbitally-induced variations in insolation are the dominant forcing mechanisms of long-term climatic variability (Kutzbach and Street-Perrot, 1985; Renssen et al., 2005a,b); these variations differ according to both season and latitude. In the Northern Hemisphere (NH), the seasonal contrast in insolation was greater during both the EH and MH than in the RT time-slice. In the NH, more insolation was received during the summer than today in the EH (between +25 and +45 W m<sup>-2</sup>), and to a lesser extent in the MH (between +10 and +25 W m<sup>-2</sup>). During the winter, less insolation was received in the NH than today in the EH (0 to -25 W m<sup>-2</sup>) and the MH (0 to -15 W m<sup>-2</sup>). For the Southern Hemisphere (SH) the seasonal contrast was smaller in the EH and MH than in the NH (Berger, 1978). Substantial alterations in land cover can significantly affect the discharge regimes of rivers (Tu, 2006). With respect to land cover changes in our study, VECODE only simulates small land cover anomalies

over the time-slices studied, except for in the Krishna, Nile and Syr Darya basins during the EH, and the Nile basin during the MH, when the crop factors (and hence the potential evapotranspiration) increase by more than 5% compared to RT. Therefore the effects of land cover change on simulated discharge will be small for the majority of the basins. If climate is the major driving force of hydrological systems (Knox, 2000), one would expect to see a response to these orbital forcings in the palaeodischarge results. Hence, we present a zonal assessment of the trends indicated by the model and proxy data.

When proxy data are discussed, dates are given using the system found in the citation, i.e. either cal. yrs. or <sup>14</sup>C yrs. are used depending on the system used in the original literature. To simplify comparison between the time-slices, approximate conversions of key dates are shown below, calculated using CalPal Online (<http://www.calpal-online.de>).

EH	9000–8650 cal. yr. BP	8100–7850 <sup>14</sup> C yr. BP
MH	6200–5850 cal. yr. BP	5400–5100 <sup>14</sup> C yr. BP

#### 4.1.1. (Sub)-tropics

In the (sub)-tropical basins influenced by NH monsoons (Ganges, Krishna, Mekong, Congo, Nile, Volta), the higher summer insolation values during the EH and (to a lesser extent) MH (Berger, 1978) led to a relative strengthening of the summer monsoon. This monsoon strengthening was caused by the preferential heating of the continents, resulting in an increased land–ocean temperature gradient (Kutzbach and Street-Perrot, 1985; Coe and Harrison, 2002; Renssen et al., 2003), and hence higher summer monsoon precipitation depths.

In southern Asia, numerous palaeoclimatic studies record an Asian summer precipitation peak between ca. 9.5 and 5.5 <sup>14</sup>C ka. BP (see Kale et al., 2003), followed by a gradual decrease until present (Overpeck et al., 1996). Regional palaeohydrological reconstructions suggest increased discharges in the EH in response to the strengthened monsoon (Kale et al., 2003). Goodbred and Kuehl (2000) state that the identification of an immense sediment flux to the floodplains and delta plains of the Ganges between ca. 11.0 and 7.0 cal. ka. BP, combined with evidence of floodplain downcutting in two upstream tributaries (Williams and Clarke, 1984), imply that Ganges discharge was much higher in the EH than at present. During the MH, sedimentation rates to the floodplain and delta plain of the Ganges were falling rapidly, but remained higher than in the RT period (Goodbred and Kuehl, 2000). Assuming similar

vegetation in the MH and RT time-slices, as suggested by pollen analysis of a peat profile from the Garhwal Himalaya (Phadtare, 2000), this suggests that discharge in the MH was similar to, or slightly higher than, discharge in the RT period. For the Krishna, radiocarbon-dated fluvial deposits provide strong evidence of increased incision and terrace formation between ca. 10.0–4.5  $^{14}\text{C}$  ka. BP (Kale and Rajaguru, 1987); the authors relate this to a period of increased river discharge. An investigation of  $\delta^{18}\text{O}$  fluctuations in a sediment core from the South China Sea found a freshwater plume from the Pearl River, representing a runoff extreme that persisted from the early Holocene until ca. 8.3 cal. ka. BP, after which time a salinity maximum ensued (Wang et al., 1999a). This suggests that the EH increase in monsoon precipitation extended to the east of the Mekong basin. Furthermore, a multi-proxy analysis of three sediment cores from the western and southern regions of the South China Sea shows a distinct  $\delta^{18}\text{O}$ -freshwater signal during the EH, which Wang et al. (1999b) tentatively link to enhanced Mekong discharge.

Proxy records for (sub)-tropical African rivers affected by monsoonal circulation (Congo, Nile, Volta) also suggest a gradual decrease of discharge from an EH peak towards RT. Such a signal is seen in the  $\delta^{18}\text{O}$  compositions of planktonic foraminifera in Congo River Fan sediment cores (Giresse and Lanfranchi, 1984; Preuss, 1990; Uliana et al., 2002). Wirmann et al. (2001) reconstructed regional environmental conditions based on an analysis of the mineral composition of Lake Ossa sediments (Cameroon), and found evidence of both decreasing discharge and precipitation since at least 5.4 cal. ka. BP. A sapropel unit (ca. 9.0–7.0 cal. ka. BP) in a cyclothem from the eastern Mediterranean reflects a significant increase in the input of less saline water from sources including the Nile (Adamson et al., 1980). Stanley (1978) attributes an isotopic change in the same period in core GA32 to an increase in both temperature and freshwater influx. The presence of a calcareous unit (ca. 3.0–0 cal. ka. BP) in the same cyclothem (Adamson et al., 1980) implies aridity in the Nile basin at that time (Stanley and Maldonado, 1977). The  $^{87}\text{Sr}/^{86}\text{Sr}$  ratio of sediments at Manzal Lagoon in the Nile Delta (Krom et al., 2002) suggests that discharge in the MH was higher than in the RT period, but lower than in the EH. Evidence of flooding, and the development of palustrine areas close to the Blue Nile riverbed prior to ca. 8.0  $^{14}\text{C}$  ka. BP, indicates humid conditions and high discharge. Stager et al. (1997) used diatom assemblages to reconstruct Holocene lake level stands of Lake Victoria, regional humidity and, to a certain degree, White Nile

discharge. Lake levels were high between ca. 11.4 and 7.9 cal. ka. BP, and became lower thereafter, culminating in the onset of arid conditions after ca. 2.3 cal. ka. BP. For the EH, Owen et al. (1982) obtained similar results for Lake Turkana, ca. 400 km to the north. No palaeodischarge data specific to the Volta were identified; hence regional proxy data have been used. Talbot and Delibrias (1980), Talbot et al. (1984) and Talbot and Johannessen (1992) reconstructed palaeohumidity from sediment cores in Lake Bosumtwi, Ghana, and found that the lake was consistently higher during the EH and MH than in the RT time-slice. An examination of diamondiferous sediments on the Birim River floodplain in Ghana suggests that discharge was high between ca. 9.0 and 7.5  $^{14}\text{C}$  ka. BP (EH), and somewhat lower thereafter (Hall et al., 1985). Reconstructions based on  $\delta^{18}\text{O}$  fluctuations in the mouth of the Niger suggest that Niger discharge was also significantly higher in the EH and MH than today (Giresse et al., 1982, cited in Preuss, 1990).

For all of the rivers discussed above, agreement was conferred between proxy and model data; monsoonal climatic and hydrological conditions appear to be well simulated. Noteworthy increases in the crop factors derived from VECODE occurred for the Nile (EH and MH) and Krishna (EH), meaning that the land cover enhanced the potential for evapotranspiration during this period. However, given the large discharge increases in the EH and MH, the increased potential for evapotranspiration (and concomitant decrease in mean discharge) does not appear to have had a dominant influence on discharge. Most of the tropical monsoon basins show slightly higher crop factors during the EH and MH compared to RT, related to increased forest cover. This may have amplified the increase in monsoonal intensity by lowering surface albedo, and consequently enhancing the preferential heating of the continents (Kutzbach and Street-Perrot, 1985; Roberts, 2002; Renssen et al., 2005a; Aerts et al., 2006).

The Zambezi lies in an area between two distinct climatic regimes: a generally wet monsoonal climate to the north, and a dry climate to the south. Lakes in tropical eastern Africa were generally higher than present during the MH, and even higher in the EH (Jolly et al., 1998). We infer that this period was wetter than the RT time-slice. A significant increase in mangrove pollen in a core from the Mozambique Channel at ca. 9.0  $^{14}\text{C}$  ka. BP suggests an increase in continental runoff and, more specifically, wetter conditions in the Zambezi Basin. However, the model simulates very large decreases in discharge during both the MH and EH. This discrepancy may be

a result of the quasi-geostrophic nature of ECBilt-CLIO-VECODE, which causes a relatively poor simulation of some tropical climates. Furthermore, since the Zambezi lies in an area surrounded by two distinct and different climatic zones, the coarse resolution of ECBilt-CLIO-VECODE may poorly resolve such abrupt geographical changes in climatic regimes.

A continuous reconstruction of Amazon Holocene discharge, based on the  $\delta^{18}\text{O}$  composition of planktonic foraminifera in sediment cores from the Amazon fan, suggests that annual discharge in the EH was ca. 93% of RT discharge, and in the MH ca. 90% of RT discharge (Maslin and Burns, 2000). Records of  $\delta^{18}\text{O}$  changes in Lake Junin (Peru) suggest a similar pattern (Seltzer et al., 2000). Van der Hammen et al. (1992) interpret periods of peat layer extension in the EH and MH on the floodplain of the Caquetá basin as periods when river discharge and flood frequency were (slightly) lower than today. Slightly lower simulated discharges for the EH (−2.4%) and MH (−0.7%) are in agreement with these findings, and can be related to fluctuations of insolation at 10°S during the SH summer. This was at a peak in the RT time-slice, almost at a Holocene low during the EH, and between these two values in the MH (Maslin and Burns, 2000). Hence, the RT period is characterised by more intense summer convection over the Amazon basin, resulting in a southward penetration of the Intertropical Convergence Zone (ITCZ), drawing in moist air from the Atlantic Ocean which is deposited over the Amazon Basin as precipitation. During periods of lower insolation at 10°S, atmospheric circulation is thought to be more zonal, preventing the summer penetration of the ITCZ over the Amazon, leading to reduced summer precipitation (Maslin and Burns, 2000). The precipitation anomaly between the time-slices in the ECBilt-CLIO-VECODE data is indeed greatest during the SH summer, lending support to insolation changes as the main causal mechanism.

#### 4.1.2. Northern hemisphere mid-latitudes

At NH mid-latitudes the annual distribution of precipitation is more even than at low-latitudes, and hence the impact of the positive summer insolation anomaly during the EH and MH on discharge should be smaller, since it is partially offset by the negative insolation anomaly in the winter (Aerts et al., 2006). This inference appears to hold true for European mid-latitude basins with (varying degrees of) maritime influence (Meuse, Rhine, Oder, Danube); proxy data for all of these basins infer similar discharges in the time-slices studied. Rotnicki (1991) applied standard

steady uniform flow formulae (*ibid*, p. 439) to the geometric characteristics of meandering palaeochannels of the Proсна River (a tributary of the Oder via the Warta in Poland), and found that discharges in the EH and MH were broadly similar to those in the RT time-slice. Howard et al. (2004) found no evidence of higher or lower discharge than today during the EH or MH in alluvial terrace sequences in the Teleorman Valley, a major Danube tributary. Becker and Schirmer (1977) found no periods of major Rann deposition (sub-fossilised oak trunk layers) on the Danube or the Main (a Rhine tributary) for the three time-slices studied, which may suggest similar discharges. It should be noted that the Main is a pluvial tributary, and therefore its pattern of discharge variation does not necessarily reflect that of the Rhine, which is partly snowmelt fed and partly pluvial (Kwadijk, 1991). Bohncke and Vandenberghe (1991) used palaeobotanical evidence and beetle remains to derive data on Holocene temperature, precipitation, and evapotranspiration in the Mark basin (southern Netherlands), close to the Meuse basin. Using these derived variables, discharge estimates were made for the period 14.0–0.5  $^{14}\text{C}$  ka. BP, suggesting that discharge was similar in the EH to the MH; no comparison was made to the RT time-slice. Similar hydrological conditions in northern Belgium during the three time-slices are inferred from palaeobotanical data in combination with data on channel pattern and depositional processes (Vandenberghe et al., 1984). For these basins the simulation results also suggest similar discharges throughout the Holocene, except for the Danube in the EH, where an increase of 12.5% was modelled compared to RT. For the latter basin our model simulated relatively high precipitation depths in the late summer during the EH and MH, perhaps related to the insolation-driven increase in precipitation seasonality as maritime influence diminishes.

In the Eurasian mid-latitude continental basins, the Volga and Syr Darya, marked precipitation seasonality exists, and hence the influence of the EH and MH positive summer insolation anomaly assumes a greater importance. Sedimentary records from the Syr Darya and Aral Sea suggest relatively low discharge prior to 10.0 cal. ka. BP, with a marked increase from ca. 9.0 cal. ka. BP. Discharge decreased greatly again from ca. 3.5 cal. ka. BP as the climate became drier (Boomer et al., 2000). Climate models estimate that the total annual discharge of all rivers to the Aral Sea in the EH and MH was 153.4 km<sup>3</sup> (Mamedov and Trofimov, 1986), compared to ca. 120 km<sup>3</sup> today (Boomer et al., 2000). Time-continuous data on Volga Holocene discharge are not available (Overeem et al., 2003).

However, since sea surface temperatures in the Barents Sea have been found to significantly predict long-term variations in CSL (Rodionov, 1994), and there is a strong feedback between Volga discharge and CSL, temperature changes inferred from the  $\delta^{18}\text{O}$  composition of the Greenland Ice Sheet Project 2 (GISP) core have been used to force Volga Holocene discharge (Overeem et al., 2003, based on the work of Tebbens et al., 2000). The simulations suggest that relative to the RT time-slice, EH discharge was higher and MH discharge was similar. These trends are reproduced by our model, and the relative increase in simulated Holocene discharge for the Syr Darya is larger than that for the Volga, again reflecting the increasing influence of the summer insolation anomaly on discharge with increasing continentality. The increased crop factor of the EH in the Volga basin does not appear to have had a major influence on the discharge regime.

For the mid-latitude North American basins, model-proxy comparison is more complicated. For the MH period, studies of palaeochannel dimensions and particle size analyses of relict flood gravels on a number of Upper Mississippi Valley (UMV) tributaries suggest that 1–2 yr flood events were larger in the MH than during the RT time-slice (Knox, 1985, 2000). Similar results were obtained by Knox (1985), based on changes in the vertical thickness of point bar sediments. The model simulates the occurrence of very high flows (i.e. floods) more often in the MH than in the RT time-slice (Fig. 5).

Therefore, as well as simulating the mean discharge trend in agreement with proxy records, the model has simulated changes in flood frequency well during the MH, adding confidence to its retrodictive capabilities. For the EH the same palaeoflood indicators were used to infer reduced discharges of the Mississippi; this is not reflected in the simulation results. The flooding characteristics of the UMV tend to show a strong correlation with continental scale shifts in tropospheric circulation. When the prevailing tropospheric circulation favours strong north-westerly or westerly airflows across the UMV region, air masses of high water-vapour content from the tropics are blocked from reaching the area and large floods are rare (Knox, 2003); this could be the mechanism responsible for reduced floods in the EH. Since ECBilt-CLIO-VECODE simulates some tropical climates relatively poorly, such weather patterns are not well resolved, and this may explain the lack of agreement during the EH. Another explanation is related to the presence of the Laurentide ice sheet in North America during the EH (Knox, 1983, 2000). This would have had a large effect on continental, regional and local weather patterns in the Upper Mississippi region. As the Laurentide ice sheet is neither modelled by ECBilt-CLIO-VECODE nor STREAM, its effects are not recorded in the simulated discharge results.

Using salinity indicators in sediment cores from the San Francisco Bay estuary, Goman and Wells (2000) found that the discharge of the Sacramento–San Joaquin

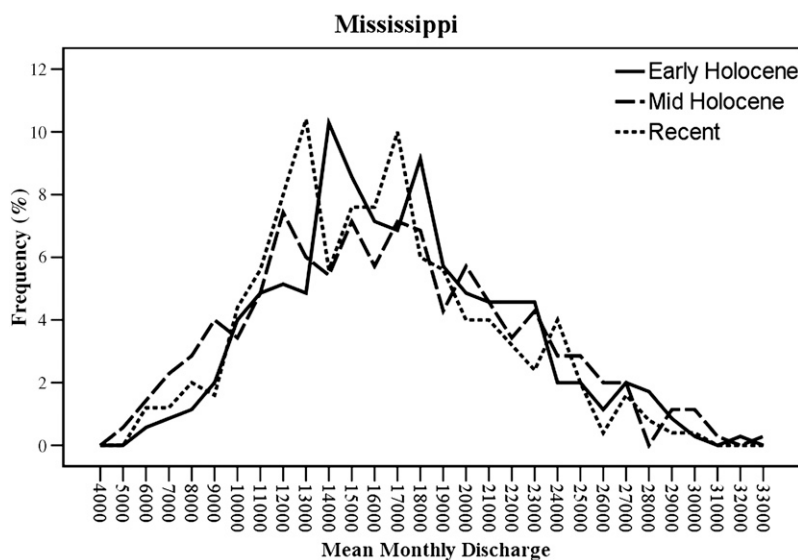


Fig. 5. Modelled mean monthly discharge ( $\text{m}^3 \text{s}^{-1}$ ) frequency distributions for the Mississippi during the Early Holocene, Mid-Holocene and Recent time-slices.

system was broadly comparable to today during the MH. Similar results were obtained by Ingram et al. (1996) based on the  $\delta^{18}\text{O}$  and  $\delta^{13}\text{C}$  compositions of fossil molluscs. This also suggests a reduced effect of insolation anomalies on discharge in these latitudes. For the EH, no specific palaeodischarge studies were identified and regional palaeoclimatological reconstructions give greatly different results for sub-regions within the basin (Heusser, 1978; Adam et al., 1981; Koehler and Scott Anderson, 1994; Davis, 1999). Hence no trend could be identified for the Sacramento–San Joaquin during the EH, and model-proxy comparison is not possible.

#### 4.1.3. Southern hemisphere mid-latitudes

Lake levels in the interior of south-eastern Australia were lower than present during the EH (Harrison and Dodson, 1993). Sediments from Lake Keilambete suggest that the lake was almost dry shortly prior to 10.0 cal. ka. BP, but that its level rose slightly between 10.0 and 8.0 cal. ka. BP. After ca. 8.0 cal. ka. BP the lake level rose rapidly, and a period of possible overflowing ensued between ca. 6.5 and 5.5 cal. ka. BP (Bowler, 1981); the simulation results for the Murray–Darling agree with these trends. Insolation anomalies during the main rainy season (September to November) were positive for both the EH and MH, and modelled precipitation in this season is higher than RT for both the EH and MH; this is counterintuitive to the discharge results. However, during the SH mid-summer, the insolation anomaly was negative during the Holocene, with a stronger negative signal and lower precipitation for the EH compared to the MH (Berger, 1978). We speculate that this combination of insolation anomalies could explain the changes in discharge trends in the model and proxy records; further research of other time-slices would be necessary to confirm this.

#### 4.1.4. Periglacial regions

In response to the NH summer insolation maximum, the EH (and to a lesser extent MH) was relatively warm and wet at northern high latitudes, especially during the summer (Renssen et al., 2005a). In the Lena basin these changes have had little impact on mean annual discharge according to both the model and proxy data. Maceral analysis of two Laptev Sea sediment cores suggests that the magnitude of river discharge to the sea remained similar throughout the Holocene (Boucein et al., 2000). A detailed Holocene environmental reconstruction of the Lena Delta area based on multi-proxy records from Nikolay Lake and a nearby peat sequence shows no evidence

of significant hydrological changes during the time-slices studied (Andreev et al., 2004). A regional review of river channel morphology in East Siberia states that there are no channel morphological indications of large-scale changes in Holocene discharge comparable to those registered for West Siberia and the Russian Plain (Sidorchuk et al., 2003). The ECBilt-CLIO-VECODE climate data for the Lena indicate that whilst summer precipitation was higher in the EH and MH, so too was temperature (and hence evapotranspiration); changes in temperature and precipitation appear to have had a compensatory effect on discharge.

Based on an investigation of the marine mollusc record for glaciated North America and Greenland, Dyke et al. (1996) suggest that large quantities of Laurentide meltwater were still entering the Mackenzie during the EH. During this time-slice the Laurentide ice sheet was still in wastage (Knox, 1983; Dyke and Prest, 1987; Knox, 2000). Given that the Laurentide ice sheet is neither modelled in the climate model nor the hydrological model, the simulated discharge for the EH was too low, since the huge meltwater component was ignored. The ice sheet would also have affected Mackenzie discharge through its effects on continental, regional and local weather patterns. According to Maizels' (1995) model of palaeodischarge in polar regions, the discharge of the Mackenzie would have been similar in magnitude to present during the MH, in agreement with the simulation results.

#### 4.2. Holocene insolation anomalies and zonal discharge trends

Clear latitudinal patterns of changes in discharge trends have been identified. An examination of the basins studied shows that these changes can be related to latitudinal and seasonal differences in insolation anomalies over the Holocene. The greatest effect is seen in the (sub)-tropical monsoon basins, where higher summer insolation during the EH (and to a lesser extent MH) caused large increases in summer precipitation and discharge. In mid-latitudes the discharge response to variations in insolation are generally less extreme, especially in maritime climates. In northern high latitudes, increased summer precipitation during the EH and MH seems to have been compensated by higher temperatures (and therefore evapotranspiration) during those periods.

In a sensitivity study of fifteen rivers, using the same model as described here, Aerts et al. (2006) compared simulated discharge trends of the last 9000 yrs with

simulated trends for the coming century. For most of the rivers studied, the change in mean simulated discharge during the next 100 yrs compared to present was greater than, or similar to, the change in simulated mean discharge over the last 9000 yrs. For the coming century their study suggests that increased atmospheric greenhouse gas concentrations will replace orbitally-induced insolation variations as the dominant forcing mechanism of global river discharge.

#### 4.3. Recommendations and applications

Since the model performs well in the majority of the basins for the time-slices studied, it is now possible to apply our approach in an operational sense. The coupled climate-hydrological model can be used to build up references of palaeodischarge over a large range of Holocene climates, or to simulate discharge under future climate change and/or land use scenarios. For water management, one of the most important uses of hydrological models is in peak flow (flood) prediction. In this study the aim was to assess the model's ability to simulate mean discharge, and not specifically flood events. To make accurate predictions of flood magnitude and frequency, modelling should take place at a higher temporal resolution. Nevertheless, the results for the Mississippi give some indication that the current model already appears to simulate changes in flood magnitude and frequency. Furthermore, when using the model to assess flood and low-flow frequencies a higher spatial resolution should be used, since daily discharge is influenced by the geographical position at which precipitation falls within a basin. The forcing parameters that were used in the climate model effect long-term (millennial) climatic fluctuations. When looking at shorter term discharge fluctuations other forcing mechanisms should be included, especially solar activity and volcanic aerosol content. In this study, Holocene land cover changes were based on the results of VECODE, which only simulates natural changes in vegetation in response to climatic change. For more detailed discharge assessments at the individual basin level, data on anthropogenic land use changes should be included (e.g. from historical, archaeological or palynological records).

The absence of the Laurentide ice sheet in our model means that the simulated discharges of North American rivers during the EH are poor. In any future application of the palaeodischarge modelling approach to North American basins it is imperative that the Laurentide ice sheet be included when considering the EH.

## 5. Conclusions

Given the level of agreement between simulated palaeodischarge and palaeodischarge as implied by the proxy records, we conclude that our coupled climate-hydrological model performs well in modelling mean annual discharge over the EH and MH time-slices. On a global scale, orbitally-induced variations in insolation are the dominant mechanism responsible for discharge changes in the time-slices studied. Furthermore, the effects of these insolation variations on discharge vary according to latitude, intuitively following latitudinal and seasonal insolation anomalies. In the coming century, increased greenhouse gas concentrations are expected to replace orbitally-induced variations in insolation as the dominant forcing mechanism of global river discharges.

In principle the palaeodischarge modelling approach has three major strengths. Firstly, palaeodischarge proxy data provide a dataset for validating model response over a longer time-period than instrumental records. Secondly, palaeodischarge models can simulate future discharge changes associated with a large range of climatic variations with more confidence than those validated against instrumental measurements only. Thirdly, the results of palaeodischarge models may provide a natural background of discharge variation with which to compare future scenarios.

Validation of palaeodischarge models can only be carried out for rivers where detailed assessments of palaeodischarge exist. For a number of the basins studied here this was not the case. Nevertheless, for those basins for which we identified good or reasonable palaeodischarge proxy data, some 72% of the runs were in good agreement with the proxy data, and 92% of the runs were in at least reasonable agreement. Furthermore, our model was able to simulate relative changes in the magnitude of palaeodischarge between the EH and MH. For those basins for which the model performed well over all three time-slices, considerable confidence is added to the model's skill compared to hydrological models validated only against the period of instrumental records.

## Acknowledgements

This research project was carried out in the framework of the Dutch National Research Programme "Climate changes Spatial Planning" ([www.klimaatvoorruijnt.nl](http://www.klimaatvoorruijnt.nl)). We would like to thank Jef Vandenbergh, Ronald van Balen and two anonymous reviewers for their useful comments, which helped to improve the paper.

## Appendix A

Details of the observed discharge datasets used for model calibration, the calibration parameters per basin, and measures of correlation between observed and modelled discharge

Basin	Period	Gauging station	Correlation tests			Calibration parameter					
			% <sup>a</sup>	<i>r</i>	<i>E</i>	Crop F	TOGW	C	Melting	WHC	HEAT
Amazon	1928–83	Obidos	100.1	0.97	0.94	0.285	0.1	4.5	10	1	1
Ganges	1965–75	Paksay	99	0.97	0.94	0.83	0.3	1.5	11	1.685	0.1
Krishna	1901–60	Vijayawada	101.3	0.93	0.85	0.39	0.1	1	10	2.5	1
Mekong	1962–87	Nakhon Phanon	99.7	0.99	0.98	1.08	0.4	1.8	12	1.75	0.8
Congo	1971–99	Brazzaville	99.7	0.9	0.55	1.1	0.6	2	1	0.1	0.8
Nile	1901–45	Assiut	100.7	0.99	0.99	12.1	0.6	1.5	10	5	1
Volta	1936–64	Senchi	100.9	0.98	0.96	2.32	0.3	1.7	10	1	1
Zambezi	1979–90	Zumbo	100.3	0.99	0.98	2.16	0.3	1.1	10	1.4	0.5
Murray–Darling	1965–84	Lock 9 Upper	100.5	0.82	0.57	0.9	0.1	1.5	10	3	1
Sacramento–San Joaquin	1948–84 <sup>b</sup>	Sacramento	100.7	0.94	0.89	18.5	0.15	2.5	10	5	1
Rhine	1936–84	Rees	100.2	0.87	0.69	0.78	0.1	5	9	0.1	1
Meuse	1911–84	Lith	100.5	0.91	0.81	0.64	0.275	4.5	10	0.1	1
Danube	1921–84	Ceatal Izmail	100.6	0.98	0.95	0.29	0.1	4	10	0.55	1
Oder	1901–86	Gozdowice	100.8	0.96	0.88	0.28	0.19	8	1	0.35	0.5
Mississippi	1965–84	Tarbet Landing	99.9	0.97	0.93	1.46	0.6	2	10	0.1	1
Syr Darya	1930–59	Tyumen Aryk	99.2	0.91	0.82	9.9	0.2	3	60	3.5	1
Volga	1901–35	Volgograd	100.2	0.96	0.91	0.48	0.2	4	9	1	1
Lena	1935–84	Kusur	99.8	0.99	0.98	0.77	0.75	2	40	1	1
Mackenzie	1966–84	Norman Wells	99.7	0.98	0.96	0.98	0.2	2	40	1	1

<sup>a</sup> Total accuracy (the mean annual observed discharge as a percentage of the mean annual modelled discharge).

<sup>b</sup> Except 1962–63 due to the building of the Red Bluff Diversion Dam.

## References

- Adam, D.P., Sims, J.D., Throckmorton, C.K., 1981. 130,000-yr continuous pollen record from Clear Lake, Lake County, California. *Geology* 9, 373–377.
- Adamson, D.A., Gasse, F., Street, F.A., Williams, M.A.J., 1980. Late Quaternary history of the Nile. *Nature* 288, 50–55.
- Aerts, J.C.J.H., Bouwer, L.M., 2002. STREAM Krishna — A Hydrological Model for the Krishna River in India, Report E-02/12. RIKZ/Coastal Zone Management Centre, The Hague, The Netherlands.
- Aerts, J.C.J.H., Droogers, P., 2004. Climate change in contrasting river basins. Adaptation Strategies for Water, Food and Environment. CABI, Wallingford, U.K.
- Aerts, J.C.J.H., Kriek, M., Schepel, M., 1999. STREAM (Spatial Tools for River Basins and Environment and Analysis of Management Options): 'Set up and requirements'. *Physics and Chemistry of the Earth. Part B: Hydrology, Oceans and Atmosphere* 24 (6), 591–595.
- Aerts, J.C.J.H., Renssen, H., Ward, P.J., De Moel, H., Odada, E., Bouwer, L., Goosse, H., 2006. Sensitivity of global river discharges under Holocene and future climate conditions. *Geophysical Research Letters* 33, L19401. doi:10.1029/2006GL027493.
- Alcamo, J., Döll, P., Henrichs, T., Kaspar, F., Lehner, B., Rösch, T., Siebert, S., 2003. Development and testing of the WaterGAP 2 global model of water use and availability. *Hydrological Sciences Journal* 48 (3), 317–337.
- Andreev, A., Tarasov, P., Schwamborn, G., Ilyashuk, B., Ilyashuk, E., Bobrov, A., Klimanov, V., Rachold, V., Hubberten, H.W., 2004. Holocene palaeoenvironmental records from Nikolay Lake, Lena River Delta, Arctic Russia. *Palaeogeography, Palaeoclimatology, Palaeoecology* 209 (1–4), 197–217.
- Amell, N.W., 1999. A simple water balance model for the simulation of streamflow over a large geographic domain. *Journal of Hydrology* 217, 314–335.
- Amell, N.W., Bates, B., Lang, H., Magnuson, J.J., Mulholland, P., Fisher, S., Liu, C., McKnight, D., Starosolszky, O., Taylor, M., Aquize, E., Arnott, S., Brakke, D., Braun, L., Chalise, S., Chen, C., Folt, C.L., Gafny, S., Hanaki, K., Hecky, R., Leavesley, G.H., Lins, H., Nemecek, J., Ramasastri, K.S., Somlyódy, L., Stakhiv, E., 1996. Hydrology and freshwater ecology. In: Watson, R.T., Zinyowera, M.C., Moss, R.H. (Eds.), *Climate Change 1995: Impacts, Adaptations and Mitigation of Climate Change: Scientific-Technical Analyses. Contribution of Working Group II to the Second Assessment Report of the Intergovernmental Panel on*

- Climate Change. Cambridge University Press, Cambridge, U.K., pp. 325–363.
- Amell, N., Liu, C., Compagnucci, R., Da Cunha, L., Hanaki, K., Howe, C., Mailu, G., Shiklomanov, I., Stakhiv, E., 2001. Hydrology and water resources. In: Houghton, J.T., Ding, Y., Griggs, D.J., Noguer, M., Van der Linden, P.J., Dai, X., Maskell, K., Johnson, C.A. (Eds.), *Climate Change 2001: Impacts, Adaptation and Vulnerability. Contribution of Working Group II to the Third Assessment Report of the Intergovernmental Panel on Climate Change*. Cambridge University Press, Cambridge and New York, pp. 193–233.
- Becker, B., Schirmer, W., 1977. Palaeoecological study on the Holocene valley development of the River Main, southern Germany. *Boreas* 6, 303–321.
- Berger, A.L., 1978. Long-term variations of daily insolation and Quaternary climatic changes. *Journal of the Atmospheric Sciences* 35, 2363–2367.
- Bohncke, S.J.P., Vandenbergh, J., 1991. Palaeohydrological development in the Southern Netherlands during the last 15000 years. In: Starkel, L., Gregory, K.J., Thornes, J.B. (Eds.), *Temperate Palaeohydrology*. John Wiley & Sons, Chichester, U.K., pp. 253–281.
- Boomer, I., Aladin, N., Plotnikov, I., Whatley, R., 2000. The palaeolimnology of the Aral Sea: a review. *Quaternary Science Reviews* 19 (13), 1259–1278.
- Boucein, B., Fahl, K., Stein, R., 2000. Variability of river discharge and Atlantic-water inflow at the Laptev Sea continental margin during the past 15,000 years: implications from maceral and biomarker records. *International Journal of Earth Sciences* 89, 578–591.
- Bouwer, L.M., Aerts, J.C.J.H., Van de Coterlet, G.M., Van de Giesen, N., Gieske, A., Mannaerts, C., 2004. Evaluating downscaling methods for preparing Global Circulation Model (GCM) data for hydrological impact modelling. In: Aerts, J.C.J.H., Droogers, P. (Eds.), *Climate Change in Contrasting River Basins. Adaptation Strategies for Water, Food and Environment*. CABI Publishing, Wallingford, U.K., pp. 25–47.
- Bowler, J.M., 1981. Australian salt lakes. A palaeohydrologic approach. *Hydrobiologia* 82, 431–444.
- Brovkin, V., Bendtsen, J., Claussen, M., Ganopolski, A., Kubatzki, C., Petoukhov, V., Andreev, A., 2002. Carbon cycle, vegetation, and climate dynamics in the Holocene: Experiments with the CLIMBER-2 model. *Global Biogeochemical Cycles* 16 (4), 1139. doi:10.1029/2001GB001662.
- Chatters, J.C., Hoover, K.A., 1986. Changing late Holocene flooding frequencies on the Columbia River, Washington. *Quaternary Research* 26 (3), 309–320.
- Christensen, N.S., Wood, A.W., Voisin, N., Lettenmaier, D.P., Palmer, R.N., 2004. The effects of climate change on the hydrology and water resources of the Colorado River basin. *Climatic Change* 62 (1–3), 337–363.
- Claussen, M., Mysak, L.A., Weaver, A.J., Crucifix, M., Fichefet, T., Loutre, M.-F., Weber, S.L., Alcamo, J., Alexeev, V.A., Berger, A., Calov, R., Ganopolski, A., Gooose, H., Lohmann, G., Lunkeit, F., Mokhov, I.I., Petoukhov, V., Stone, P., Wang, Z., 2002. Earth system models of intermediate complexity: closing the gap in the spectrum of climate system models. *Climate Dynamics* 18, 579–586.
- Cocke, S., LaRow, T.E., 2000. Seasonal predictions using a regional spectral model embedded within a coupled ocean-atmosphere model. *Monthly Weather Review* 128, 689–708.
- Coe, M.T., Harrison, S.P., 2002. The water balance of northern Africa during the Mid-Holocene: an evaluation of the 6 ka BP PMIP simulations. *Climate Dynamics* 19, 155–166.
- Davis, O.K., 1999. Pollen analysis of Tulare Lake, California: Great Basin-like vegetation in Central California during the full-glacial and early Holocene. *Review of Palaeobotany and Palynology* 107 (3–4), 249–257.
- Döll, P., Kaspar, F., Lehner, B., 2003. A global hydrological model for deriving water availability indicators: model tuning and validation. *Journal of Hydrology* 270, 105–134.
- Dyke, A.S., Prest, V.K., 1987. Late Wisconsin and Holocene history of the Laurentide Ice Sheet. *Géographie Physique et Quaternaire* 41 (2), 237–263.
- Dyke, A.S., Dale, J.E., McNeely, R.N., 1996. Marine molluscs as indicators of environmental change in glaciated North America and Greenland during the last 18000 years. *Géographie Physique et Quaternaire* 50 (2), 125–184.
- Ely, L.L., Enzel, Y., Baker, V.R., Cayan, D.R., 1993. A 5000-year record of extreme floods and climate change in the south-western United States. *Science* 262 (5132), 410–412.
- ESRI, 1992. *Global topographic database ArcWorld 1:3M on CDROM*. Environmental Systems Research Institute, Inc. (ESRI), Redlands, CA.
- Giresse, P., Lanfranchi, R., 1984. Les climats et les océans de la région Congolaise pendant l'Holocène-Bilans selon les échelles et les méthodes de l'observation. In: Coetzee, J.A., Van Zinderen Bakker Sr. Sr., E.M. (Eds.), *Palaeoecology of Africa*, vol. 16. A.A. Balkema, Rotterdam, The Netherlands, pp. 77–88.
- Goman, M., Wells, L., 2000. Trends in river flow affecting the north-eastern reach of the San Francisco Bay estuary over the past 7000 years. *Quaternary Research* 54 (2), 206–217.
- Goodbred, S.L., Kuehl, S.A., 2000. Enormous Ganges–Brahmaputra sediment discharge during strengthened early Holocene monsoon. *Geology* 28 (12), 1083–1086.
- Gooose, H., Fichefet, T., 1999. Importance of ice–ocean interactions for the global ocean circulation: a model study. *Journal of Geophysical Research—Oceans* 104 (C10), 23 337–23 355.
- Gooose, H., Renssen, H., Timmermann, A., Bradley, R.S., 2005. Internal and forced climate variability during the last millennium: a model-data comparison using ensemble simulations. *Quaternary Science Reviews* 24 (12–13), 1345–1360.
- Hall, A.M., Thomas, M.F., Thorp, M.B., 1985. Late Quaternary alluvial placer development in the humid tropics: the case of the Birim Diamond Placer, Ghana. *Journal of the Geological Society* 142, 777–787.
- Harrison, S.P., Dodson, J., 1993. Climates of Australia and New Guinea since 18,000 yr B.P. In: Wright Jr., H.E., Kutzbach, J.E., Webb III, T., Ruddiman, W.F., Street-Perrott, F.A., Bartlein, P.J. (Eds.), *Global Climates Since the Last Glacial Maximum*. University of Minnesota Press, Minneapolis, pp. 265–293.
- Henderson-Sellers, A., McGuffie, K., Pitman, A.J., 1996. The project for intercomparison of land-surface parameterization schemes (PILPS): 1992 to 1995. *Climate Dynamics* 12, 849–859.
- Heusser, L., 1978. Pollen in Santa Barbara Basin, California: A 12,000-yr record. *Geological Society of America Bulletin* 89, 673–678.
- Hipel, K.W., McLeod, A.I., 1994. *Time Series Modelling of Water Resources and Environmental Systems*. Elsevier, Amsterdam, The Netherlands.
- Howard, A.J., Macklin, M.G., Bailey, D.W., Mills, S., Andreescu, R., 2004. Late-glacial and Holocene river development in the Teleorman Valley on the southern Romanian Plain. *Journal of Quaternary Science* 19 (3), 271–280.
- Ingram, B.L., Ingle, J.C., Conrad, M.E., 1996. Stable isotope record of late Holocene salinity and river discharge in San Francisco Bay, California. *Earth and Planetary Science Letters* 141 (1–4), 237–247.

- IPCC, 2001. *Climate Change 2001: The Scientific Basis*. Contribution of Working Group I to the Third Assessment Report of the Intergovernmental Panel on Climate Change. Cambridge University Press, Cambridge and New York.
- Jolly, D., Harrison, S.P., Damnati, B., Bonnefille, R., 1998. Simulated climate and biomes of Africa during the Late Quaternary: comparison with pollen and lake status data. *Quaternary Science Reviews* 17 (6–7), 629–657.
- Kale, V.S., Rajaguru, S.N., 1987. Late Quaternary alluvial history of the north-western Deccan upland region. *Nature* 325 (12), 612–614.
- Kale, V.S., Gupta, A., Singhvi, A.K., 2003. Late Pleistocene–Holocene palaeohydrology of Monsoon Asia. In: Gregory, K.J., Benito, G. (Eds.), *Palaeohydrology: Understanding Global Change*. John Wiley & Sons, Chichester, U.K., pp. 213–232.
- Kim, J., Miller, N.L., Farrara, J.D., Hong, S.-Y., 2000. A seasonal precipitation and stream flow hindcast and prediction study in the western United States during the 1997/98 winter season using a dynamic downscaling system. *Journal of Hydrometeorology* 1 (4), 311–329.
- Kleinn, J., Frei, C., Gurtz, J., Lüthi, D., Vidale, P.L., Schär, C., 2005. Hydrologic simulations in the Rhine basin driven by a regional climate model. *Journal of Geophysical Research* 110, D04102. doi:10.1029/2004JD005143.
- Klepper, O., Van Drecht, G., 1998. Waribas, Water Assessment on a River Basin Scale: A Computer Program for Calculating Water Demand and Water Satisfaction on a Catchment Basin Level for Global-Scale Analysis of Water Stress. Report 402.001.009. RIVM, Bilthoven, The Netherlands.
- Knox, J.C., 1983. Responses of river systems to Holocene climates. In: Wright Jr. Jr., H.E. (Ed.), *Late-Quaternary Environments of the United States*, vol. 2. Longman, London, U.K., pp. 26–41.
- Knox, J.C., 1985. Responses of floods to Holocene climatic change in the Upper Mississippi Valley. *Quaternary Research* 23 (3), 287–300.
- Knox, J.C., 2000. Sensitivity of modern and Holocene floods to climate change. *Quaternary Science Reviews* 19 (1–5), 439–457.
- Knox, J.C., 2003. North American palaeofloods and future floods: responses to climatic change. In: Gregory, K.J., Benito, G. (Eds.), *Palaeohydrology. Understanding Global Change*. John Wiley & Sons, Chichester, U.K., pp. 143–164.
- Koehler, P.A., Scott Anderson, R., 1994. The paleoecology and stratigraphy of Nichols Meadow, Sierra National Forest, California, USA. *Palaeogeography, Palaeoclimatology, Palaeoecology* 112 (1–2), 1–17.
- Krom, M.D., Stanley, J.D., Cliff, R.A., Woodward, J.C., 2002. Nile River sediment fluctuations over the past 7000 yr and their key role in sapropel development. *Geology* 30 (1), 71–74.
- Kutzbach, J., Street-Perrot, F.A., 1985. Milancovitch forcing of fluctuations in the level of tropical lakes from 18 to 0 kyr BP. *Nature* 317, 130–134.
- Kwadijk, J.C.J., 1991. Sensitivity of the River Rhine discharge to environmental change, a first tentative assessment. *Earth Surface Processes and Landforms* 16, 627–637.
- Kwadijk, J.C.J., 1993. *The Impact of Climate Change on the Discharge of the River Rhine*. PhD Thesis, University of Utrecht, Utrecht, The Netherlands.
- Legates, D.R., McCabe Jr., G.J., 1999. Evaluating the use of “goodness-of-fit” measures in hydrologic and hydroclimatic model validation. *Water Resources Research* 35 (1), 233–241.
- Maizels, J.K., 1995. Palaeohydrology of polar and subpolar regions over the past 20,000 years. In: Gregory, K.J., Starkel, L., Baker, V.R. (Eds.), *Global Continental Palaeohydrology*. John Wiley & Sons, Chichester, U.K., pp. 259–299.
- Mamedov, E.D., Trofimov, G.N., 1986. On the problem of long-term oscillations of the Central Asian rivers. *Problemy Osvoenia Pustyn* 1, 12–16 (in Russian).
- Maslin, M.A., Burns, S.J., 2000. Reconstruction of the Amazon basin effective moisture availability over the past 14,000 years. *Science* 290 (5500), 2285–2287.
- Meybeck, M., 2003. Global analysis of river systems: from Earth system controls to Anthropocene syndromes. *Philosophical Transactions - Royal Society. Biological Sciences* 358, 1935–1955.
- Mitchell, T.D., Carter, T.R., Hulme, M., New, M., 2003. A comprehensive set of high-resolution grids of monthly climate for Europe and the globe: the observed record (1901–2000) and 16 scenarios (2001–2100). Tyndall Centre Working Paper, vol. 55. Tyndall Centre for Climate Change Research, Norwich, U.K.
- Moy, C.M., Seltzer, G.O., Rodbell, D.T., Anderson, D.M., 2002. Variability of El Niño/Southern Oscillation activity at millennial timescales during the Holocene epoch. *Nature* 420, 162–165.
- Murphy, J., 2000. Predictions of climate change over Europe using statistical and dynamical downscaling techniques. *International Journal of Climatology* 20 (5), 489–501.
- Nash, J.E., Sutcliffe, J.V., 1970. River flow forecasting through conceptual models, A discussion of principles. *Journal of Hydrology* 10, 282–290.
- NGDC, 1997. Terrain Base: Global 5 min. elevation database. National Geophysical Data Center, Washington. [www.ngdc.noaa.gov](http://www.ngdc.noaa.gov).
- Opsteegh, J.D., Haarsma, R.J., Selten, F.M., Kattenberg, A., 1998. ECBILT: a dynamic alternative to mixed boundary conditions in ocean models. *Tellus* 50A, 348–367.
- Overeem, I., Veldkamp, A., Tebbens, L., Kroonenberg, S.B., 2003. Modelling Holocene stratigraphy and depocentre migration of the Volga delta due to Caspian Sea-level change. *Sedimentary Geology* 159 (3–4), 159–175.
- Overpeck, J., Anderson, D., Trumbore, S., Prell, W., 1996. The southwest Indian Monsoon over the last 18000 years. *Climate Dynamics* 12 (3), 213–225.
- Owen, R.B., Barthelme, J.W., Renaut, R.W., Vincens, A., 1982. Paleolimnology and archaeology of Holocene deposits northeast of Lake Turkana, Kenya. *Nature* 298, 523–529.
- Pfister, L., Kwadijk, J., Musy, A., Bronstert, A., Hoffmann, L., 2004. Climate change, land use change and runoff prediction in the Rhine–Meuse basins. *River Research and Applications* 20, 229–241.
- Phadtare, N.R., 2000. Sharp decrease in summer monsoon strength 4000–3500 cal yr B.P. in the Central Higher Himalaya of India based on pollen evidence from Alpine peat. *Quaternary Research* 53 (1), 122–129.
- Preuss, J., 1990. L'évolution des paysages du bassin intérieur du Zaïre pendant les quarante derniers millénaires. In: Lanfranchi, R., Schwartz, D. (Eds.), *Paysages Quaternaires de l'Afrique Centrale Atlantique*. Editions de l'Ostrom, Paris, France, pp. 260–270.
- Renssen, H., Knoop, J.M., 2000. A global river routing network for use in hydrological modelling. *Journal of Hydrology* 230 (3–4), 230–243.
- Renssen, H., Brovkin, V., Fichefet, T., Goosse, H., 2003. Holocene climate instability during the termination of the African Humid Period. *Geophysical Research Letters* 30 (4), 1184–1187.
- Renssen, H., Goosse, H., Fichefet, T., Brovkin, V., Driesschaert, E., Wolk, F., 2005a. Simulating the Holocene climate evolution at northern high latitudes using a coupled atmosphere–sea–ice–ocean–vegetation model. *Climate Dynamics* 24 (1), 23–43.

- Renssen, H., Goosse, H., Fichet, T., Masson-Delmotte, V., Koç, N., 2005b. The Holocene climate evolution in the high-latitude Southern Hemisphere simulated by a coupled atmosphere–sea ice–ocean–vegetation model. *Holocene* 15, 951–964.
- Roberts, N., 2002. *The Holocene— An Environmental History*. Blackwell, Oxford, U.K.
- Rodionov, S.G., 1994. *Global and Regional Climate Interaction: The Caspian Sea Experience*. Kluwer Academic Publishing, Dordrecht, The Netherlands.
- Rotnicki, K., 1991. Retrodiction of palaeodischarges of meandering and sinuous alluvial rivers and its palaeoclimatic implications. In: Starkel, L., Gregory, K.J., Thomes, J.B. (Eds.), *Temperate Palaeohydrology. Fluvial Processes in the Temperate Zone during the last 15000 years*. John Wiley & Sons, Chichester, U.K., pp. 431–471.
- Seltzer, G., Rodbell, D., Burns, S.J., 2000. Isotopic evidence for late Quaternary climatic change in tropical South America. *Geology* 28 (1), 35–38.
- Sidorchuk, A., Panin, A., Borisova, O., 2003. The Lateglacial and Holocene palaeohydrology of Northern Eurasia. In: Gregory, K.J., Benito, G. (Eds.), *Palaeohydrology: Understanding Global Change*. John Wiley & Sons, Chichester, U.K., pp. 61–76.
- Stager, J.C., Cumming, B., Meeker, L., 1997. A high-resolution 11,400-yr diatom record from Lake Victoria, East Africa. *Quaternary Research* 47 (1), 81–89.
- Stanley, J.D., 1978. Ionian Sea sapropel distribution and late Quaternary palaeoceanography in the eastern Mediterranean. *Nature* 274, 149–152.
- Stanley, J.D., Maldonado, A., 1977. Nile Cone: Late Quaternary stratigraphy and sediment dispersal. *Nature* 266, 129–135.
- Talbot, M.R., Delibrias, G., 1980. A new late Pleistocene–Holocene water level curve for Lake Bosumtwi, Ghana. *Earth and Planetary Science Letters* 47, 336–344.
- Talbot, M.R., Johannessen, T., 1992. A high resolution palaeoclimatic record for the last 27,500 years in tropical West Africa from the carbon and nitrogen isotopic composition of lacustrine organic matter. *Earth and Planetary Science Letters* 110, 23–37.
- Talbot, M.R., Livingstone, D.A., Palmer, P.G., Maley, J.M., Delibrias, G., Gulliksen, S., 1984. Preliminary results from sediment cores from Lake Bosumtwi, Ghana. In: Coetzee, J.A., Van Zinderen Bakker Sr. Sr., E.M. (Eds.), *Palaeoecology of Africa*, vol. 16. A.A. Balkema, Rotterdam, The Netherlands, pp. 173–192.
- Tebbens, L.A., Veldkamp, A., Van Dijke, J.J., Schoorl, J.M., 2000. Modelling longitudinal profile development in response to Late Quaternary tectonics, climate and sea level changes: the River Meuse. *Global and Planetary Change* 27 (1–4), 165–186.
- Thornthwaite, C.W., 1948. An approach toward a rational classification of climate. *The Geographical Review* 38, 55–94.
- Thornthwaite, C.W., Mather, J.R., 1957. *Instructions and tables for computing potential evapotranspiration and the water balance*. *Publications in Climatology* 10, 183–243.
- Tu, M., 2006. *Assessment of the effects of climate variability and land use change on the hydrology of the Meuse river basin*. PhD Thesis, Vrije Universiteit Amsterdam and UNESCO-IHE Delft, The Netherlands.
- Uliana, E., Lange, C.B., Wefer, G., 2002. Evidence for Congo River freshwater load in Late Quaternary sediments of ODP Site 1077 (5°S, 10 °E). *Palaeogeography, Palaeoclimatology, Palaeoecology* 187 (1–2), 137–150.
- Vandenbergh, J., Paris, P., Kasse, C., Gouman, M., Beyens, L., 1984. Paleomorphological and botanical evolution of small lowland valleys. A case study of the Mark Valley in Northern Belgium. *CATENA* 11, 229–238.
- Van der Hammen, T., Urrego, L.E., Espejo, N., Duivenvoorden, J.F., Lips, J.M., 1992. Late-glacial and Holocene sedimentation and fluctuations of river water level in the Caquetá River area (Colombian Amazonia). *Journal of Quaternary Science* 7 (1), 57–67.
- Van Deursen, W.P.A., 1995. *Geographical Information Systems and Dynamic Models*. PhD Thesis, University of Utrecht, Utrecht, The Netherlands.
- Van Deursen, W.P.A., Kwadijk, J.C.J., 1994. *The impacts of climate change on the water balance of the Ganges–Brahmaputra and Yangtze basin*. Report number RA/94-160, Resource Analysis, Delft, The Netherlands.
- Vörösmarty, C.J., Fekete, B.M., Tucker, B.A., 1998. *Global River Discharge, 1807–1991, V[ersion] 1.1 (RivDis)*. Oak Ridge National Laboratory Distributed Active Archive Center, Oak Ridge, TN. <http://www.daac.ornl.gov>.
- Wang, L., Sarnthein, M., Erlenkeuser, H., Grootes, P., Grimalt, J.O., Pelejero, C., Linck, G., 1999a. Holocene variations in Asian monsoon moisture: a bidecadal sediment record from the South China Sea. *Geophysical Research Letters* 26 (18), 2889–2892.
- Wang, L., Sarnthein, M., Erlenkeuser, H., Grimalt, J., Grootes, P., Heilig, S., Ivanova, E., Kienast, M., Pelejero, C., Pflaumann, U., 1999b. East Asian monsoon climate during the Late Pleistocene: high-resolution sediment records from the South China Sea. *Marine Geology* 156, 245–284.
- Wilby, R.L., Wigley, T.M.L., 1997. Downscaling general circulation model output: a review of methods and limitations. *Progress in Physical Geography* 21 (4), 530–548.
- Wilby, R.L., Wigley, T.M.L., Conway, D., Jones, P.D., Hewitson, B.C., Main, J., Wilks, D.S., 1998. Statistical downscaling of general circulation model output: a comparison of methods. *Water Resources Research* 34 (11), 2995–3008.
- Wilby, R.L., Hay, L.E., Gutowski Jr., W.J., Arritt, R.W., Takle, E.S., Pan, Z., Leavesley, G.H., Clark, M.P., 2000. Hydrological responses to dynamically and statistically downscaled climate model output. *Geophysical Research Letters* 27 (8), 1199–1202.
- Williams, M.A.J., Clarke, M.F., 1984. Late Quaternary environments in north-central India. *Nature* 308 (12), 633–635.
- Wirmann, D., Bertaux, J., Kossoni, A., 2001. Late Holocene paleoclimatic changes in Western Central Africa inferred from mineral abundance in dated sediments from Lake Ossa (Southwest Cameroon). *Quaternary Research* 56, 275–289.
- Wood, A.W., Maurer, E.P., Kumar, A., Lettenmaier, D.P., 2002. Long-range experimental hydrologic forecasting for the eastern United States. *Journal of Geophysical Research* 107 (D20), 4429. doi:10.1029/2001JD000659.
- Wood, A.W., Leung, L.R., Sridhar, V., Lettenmaier, D.P., 2004. Hydrologic implications of dynamical and statistical approaches to downscaling climate model outputs. *Climatic Change* 62 (1–3), 189–216.
- Yarnal, B., Lakhtakia, M.N., Yu, Z., White, R.A., Pollard, D., Miller, D.A., Lapenta, W.M., 2000. A linked meteorological and hydrological model system: the Susquehanna River Basin Experiment (SRBEX). *Global and Planetary Change* 25 (1–2), 149–161.
- Yates, D.N., 1997. Approaches to continental scale runoff for integrated assessment models. *Journal of Hydrology* 201, 289–310.